

LETTER TO THE EDITOR

CMR Effect in Electron-Doped Manganites $\text{Ca}_{1-x}\text{Sm}_x\text{MnO}_3$

C. Martin, A. Maignan, F. Damay, M. Hervieu, and B. Raveau

Laboratoire CRISMAT, UMR 6508 associée au CNRS, ISMRA, et Université de Caen, 6, Boulevard du Maréchal Juin, 14050 Caen Cedex, France

Communicated by J. M. Honig, October 2, 1997; accepted October 11, 1997

The magnetic and transport properties of the Mn(IV)-rich perovskites $\text{Ca}_{1-x}\text{Sm}_x\text{MnO}_3$ have been investigated for $x \leq 0.20$. These compounds exhibit very unusual magnetic behavior, especially for $0.14 \leq x \leq 0.20$, where a peak is observed on the $M(T)$ curves, whose temperature T_{peak} increases with x , whereas their height decreases. Moreover, colossal magnetoresistance properties are exhibited for the first time in these electron-doped systems, as shown for $x = 0.15$, which exhibits resistance ratios R_0/R_{7T} , of 10^2 and 10 at 50 and 100 K, respectively. These properties are interpreted in terms of a competition between ferromagnetism and antiferromagnetism, in connection with two opposing factors, namely, electron delocalization and charge ordering. © 1997 Academic Press

Recent studies of the manganese perovskites have shown that one can induce colossal magnetoresistance (CMR) properties in lanthanide manganites LnMnO_3 by hole doping. In these systems, starting from the electronic configuration of Mn(III), $(t_{2g})^3(e_g)^1$, mobile holes are created in the e_g band of manganese, either by partly replacing the lanthanide element with a divalent cation A , according to the formula $\text{Ln}_{1-x}\text{A}_x\text{MnO}_3$ (1–7), or by introducing a lanthanide deficiency, as in $\text{La}_{1-x}\text{MnO}_3$ (8,9). The realization of such properties requires a high Mn(III) content, i.e., a lanthanide-rich composition, in order to avoid the charge ordering phenomena that appear for the oxides $\text{Ln}_{0.5}\text{A}_{0.5}\text{MnO}_3$ (10,11).

In contrast, no CMR effect has been noted to date in Mn(IV)-rich manganites, i.e., manganites containing only a few percent of lanthanide. The investigation of such compounds should be fruitful since they correspond to the doping of a Mn(IV) insulating matrix by electrons, so that a transition toward a metallic or semimetallic state should be induced. The recent evidence for large negative magnetoresistance in $\text{Bi}_{1-x}\text{Ca}_x\text{MnO}_3$ (12), although modest compared to lanthanide manganites, i.e., $R_0/R_{7T} \sim 3$ at 50 K, is in agreement with this viewpoint. For this reason we

have revisited the $\text{LnMnO}_3\text{--CaMnO}_3$ system on the calcium-rich side. In the present letter, we report on the electron-doped manganites $\text{Ca}_{1-x}\text{Sm}_x\text{MnO}_3$ ($0 < x \leq 0.20$) that exhibit a semimetallic to insulating transition in the temperature range $100\text{--}150$ K, together with an induced ferromagnetic component at low temperature, so that CMR properties with resistance ratios R_0/R_{7T} larger than 10^2 can be obtained at 50 K.

The oxides $\text{Ca}_{1-x}\text{Sm}_x\text{MnO}_3$ were prepared from mixtures of CaO , Sm_2O_3 , and MnO_2 heated at 1000°C in air, pressed into the form of bars, heated at 1200°C , and then sintered 12 h at 1500°C . The purity, homogeneity, and composition of the samples were checked by X-ray diffraction, electron diffraction, and EDS analysis.

Resistivity measurements (four-probe method) were performed with a physical properties measurement system (PPMS, Quantum Design), on $2 \times 2 \times 10$ mm bars, so that the resistivity $\rho(\Omega\cdot\text{cm}) = 10^{-1} \times R(\Omega)$. Curves were obtained on cooling, the 7-T magnetic field being applied at 300 K. Magnetization measurements were obtained by means of a SQUID magnetometer.

The magnetization curves $M(T)$ in a magnetic field of 1.45 T (Fig. 1) show that for low x values ($0 < x \leq 0.12$) a ferromagnetic state is induced at low temperature, i.e., for $T \leq 100$ K. The corresponding $R(T)$ curves (Fig. 2) clearly establish that, for this composition range, the resistance of the samples is significantly decreased with respect to that of CaMnO_3 , tending toward semimetallic behavior between 110 and 300 K, for x ranging from 0.075 to 0.12 . The properties of this first series of samples can be explained by the fact that doping with samarium introduces mobile electrons into the e_g band, so that the interaction of these carriers via t_{2g} spins induces ferromagnetic coupling. The tendency to exhibit a transition toward a ferromagnetic metallic state is clearly seen by the anomaly in the $R(T)$ curve of the $x = 0.1$ sample (inset Fig. 2), which appears at $T_C = 110$ K, in agreement with the $M(T)$ curve (Fig. 1).

For higher x values ($0.14 \leq x < 0.20$) the $M(T)$ curves are quite unusual (Fig. 1). One observes an abrupt collapse

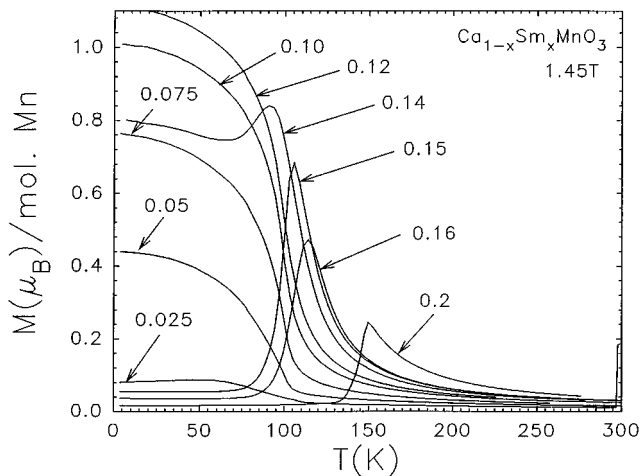


FIG. 1. Temperature dependence of the magnetization M registered under 1.45 T for the series $\text{Ca}_{1-x}\text{Sm}_x\text{MnO}_3$ (x values are labeled on the graph).

of the magnetic moment at low temperature, for x larger than 0.14, indicating a return to the antiferromagnetic state for $T < 100$ K. But the most striking feature concerns the $M(T)$ peak, which is rather sharp for $0.15 \leq x \leq 0.20$. This phenomenon, also observed for $\text{Bi}_{0.2}\text{Ca}_{0.8}\text{MnO}_3$ (12, 13) for x ranging from 0 to 0.25, can be explained by competition between electron delocalization and charge ordering. The introduction of electrons at the e_g level of Mn(III) favors electron delocalization and consequently induces the ferromagnetic component. By contrast the tendency to charge ordering and consequently to antiferromagnetism is favored as x increases and approaches $x = 0.25$, in agreement with the neutron diffraction study previously made for $(\text{La}, \text{Ca})\text{MnO}_3$ (14). The competition between these two opposing effects favors electronic delocalization for low x values (far from $x = 0.25$), leading to ferromagnetism, whereas charge ordering becomes predominant for higher x values, i.e., as x tends to 0.25, leading to antiferromagnetism. The increase of the T_{peak} from 105 K for $x = 0.15$ to 150 K for $x = 0.20$ and the decrease of the peak intensity as x increases is thus easily explained by a rapid expansion of the antiferromagnetic state (charge ordering) at the expense of ferromagnetism (electronic delocalization). The $R(T)$ curves observed for $x = 0.14$ and 0.20 (Fig. 2) are also in agreement with this interpretation: they show a transition (at 100 and 150 K) from a semimetallic to a semiconducting state as T decreases, similar to that observed in the charge-ordered manganites $\text{Ln}_{0.5}\text{A}_{0.5}\text{MnO}_3$ (10, 11).

The $R(T)$ curves in a 7 T magnetic field (Fig. 3) exhibit negative magnetoresistance over the whole domain $0 < x \leq 0.20$. The low x values $0 < x < 0.12$, which exhibit a ferromagnetic transition, are characterized by small

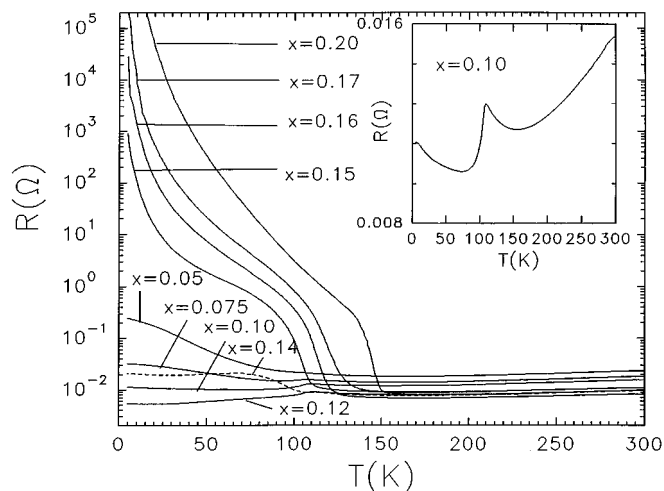


FIG. 2. Temperature dependence of the resistance R for the series $\text{Ca}_{1-x}\text{Sm}_x\text{MnO}_3$ (x values are labeled on the graph). Inset: Enlargement of the $x = 0.1$ curve.

magnetoresistance ratios R_0/R_{7T} , ranging from 1.8 for $x = 0.05$ (Fig. 3a) to 1.5 for $x = 0.10$ (Fig. 3b) at 50 K. Such a small effect is comparable to that described for the bismuth manganite $\text{Bi}_{1-x}\text{Ca}_x\text{MnO}_3$ (12), for which a resistance ratio (RR) of 3 is observed at 50 K. This can be explained by the fact that the resistance in the ferromagnetic state and near the ferromagnetic state (i.e., above T_C) is rather low, so that the application of a magnetic field cannot dramatically modify the resistance. In contrast, as soon as we reach the peak region on the $M(T)$ curves, i.e., $0.14 \leq x < 0.20$, involving a competition between ferromagnetism and antiferromagnetism, much higher RR are obtained. The RR value increases to 6 at 50 K for $x = 0.14$ (Fig. 3c), whereas the sample $x = 0.15$ exhibits CMR with resistance ratios of 10^2 at 50 K and larger than 10 at 100 K (Fig. 3d). A further increase of x leads to a decrease of RR at 50 K, as shown for $x = 0.16$ (Fig. 3e) and $x = 0.17$ (Fig. 3f) for which the RR is equal to 10 and 3 at 50 K respectively. Note, however that the RR at 110 K (near the $M(T)$ peak) of the two latter samples are still high, i.e., 15 and 7 respectively. Finally, for $x = 0.20$, the magnetoresistance effect completely disappears below 120 K, but the resistance ratio still remains high, close to 10, around 140 K, the temperature which corresponds to the $M(T)$ peak (Fig. 3g). The phases $\text{Ca}_{1-x}\text{Sm}_x\text{MnO}_3$ are very similar to the charge-ordered manganites $\text{Ln}_{0.5}\text{A}_{0.5}\text{MnO}_3$ (10, 11) which also exhibit CMR properties, in connection with the ferromagnetic metallic to antiferromagnetic insulating transition at low temperature. However in the latter, a much larger interpolated cation is required for the appearance of such an effect, since, for example, the manganite $\text{Ca}_{0.5}\text{Pr}_{0.5}\text{MnO}_3$ does not exhibit any CMR effect below

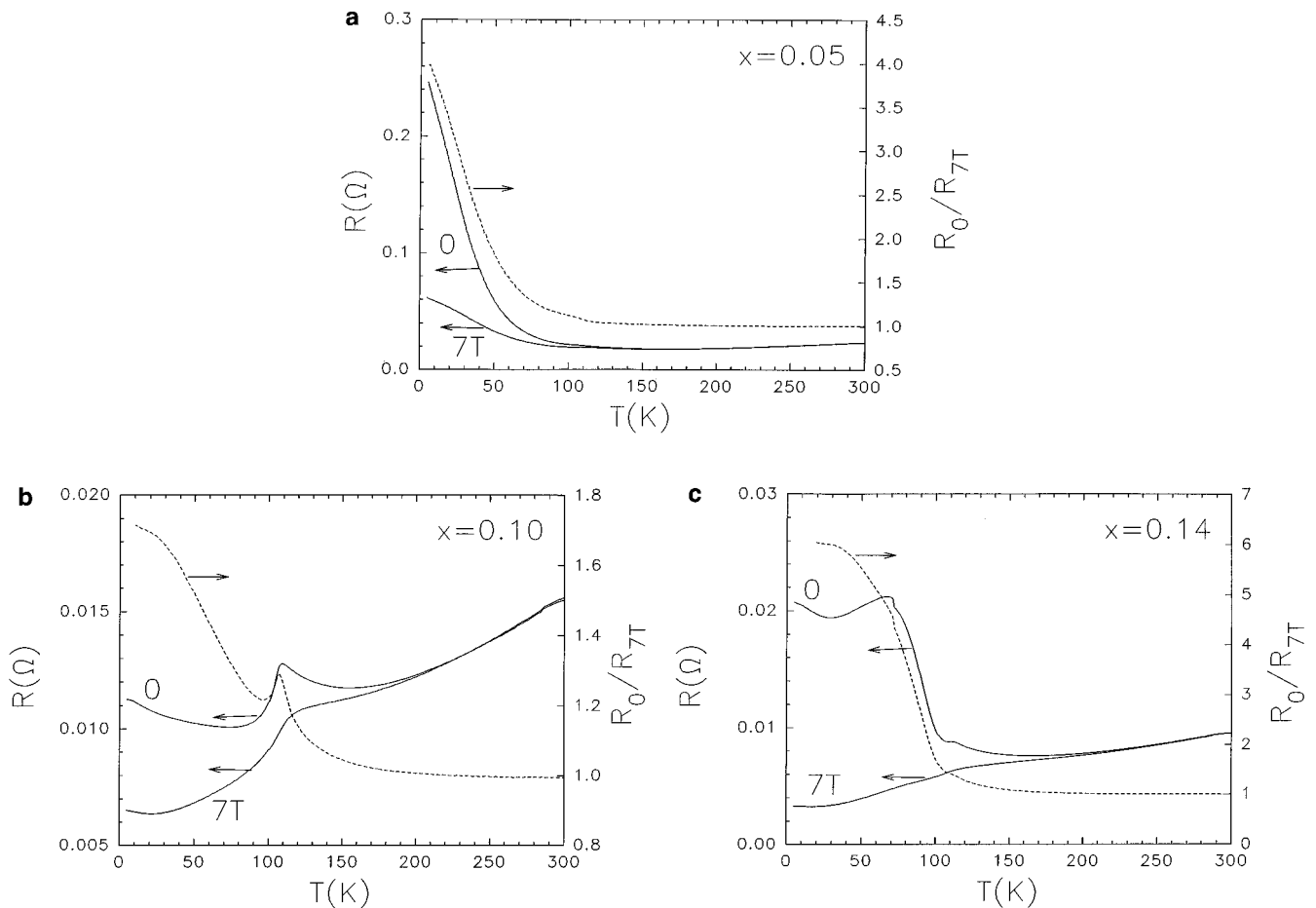


FIG. 3. $R(T)$ curves registered under 0 and 7 T (left axis) and $R_{B=0}/R_{B=7T}$ ratio (right axis) for the series $\text{Ca}_{1-x}\text{Sm}_x\text{MnO}_3$ with $x = 0.05$ (a), $x = 0.1$ (b), $x = 0.14$ (c), $x = 0.15$ (d), $x = 0.16$ (e), $x = 0.17$ (f), $x = 0.2$ (g).

7 T. Moreover, it is remarkable that the pure ferromagnetic metallic state is in fact not observed in the electron-doped manganites $\text{Ca}_{1-x}\text{Sm}_x\text{MnO}_3$. Consequently, it can be stated that the presence of ferromagnetic interactions within an antiferromagnetic insulating matrix is sufficient to induce the CMR effect.

Inspection of half-hysteresis loops registered at 10 and 100 K for $\text{Ca}_{0.85}\text{Sm}_{0.15}\text{MnO}_3$, which is the most CMR compound, is very instructive (Fig. 4). At 10 K (Fig. 4a) the magnetization values are limited to less than $0.12 \mu_B$ per Mn. The first magnetization curve, with an abrupt increase below 0.2 T indicating the existence of a weak ferromagnetic component, shows only a slight upturn for magnetic fields higher than 3 T. At this temperature, the sample is thus an antiferromagnet with a weak ferromagnetic component strengthened by the magnetic field. The slight change of the slope observed for $H > 3$ T induces irreversible modifications of the $M(H)$ loops, leading to higher M values for the

decreasing branch of the magnetic field. As T is increased, the effectiveness of the magnetic field in inducing a ferromagnetic component increases. On the $M(H)$ half-loop registered at 100 K (Fig. 4b), one can see that the magnetization reaches values up to $0.8 \mu_B/\text{Mn}$ in 5 T. Here again, hysteresis exists for the largest magnetic field values, but in low magnetic fields ($H \leq 0.2$ T) the curves become reversible, so that the sample state is not modified after a complete cycle, in contrast to the behavior observed at 10 K. Finally, it appears thus that the magnetic behavior of this CMR compound is that of an antiferromagnet, where a weak ferromagnetic component exists, so that it can be considered as a ferrimagnet. The application of a magnetic field tends to reinforce the ferromagnetic component at the expense of antiferromagnetism; this effect is amplified as the temperature is increased. Nevertheless, the lack of magnetization saturation even in 5 T and at $T = 100$ K suggests that higher magnetic fields are required to reach the expected

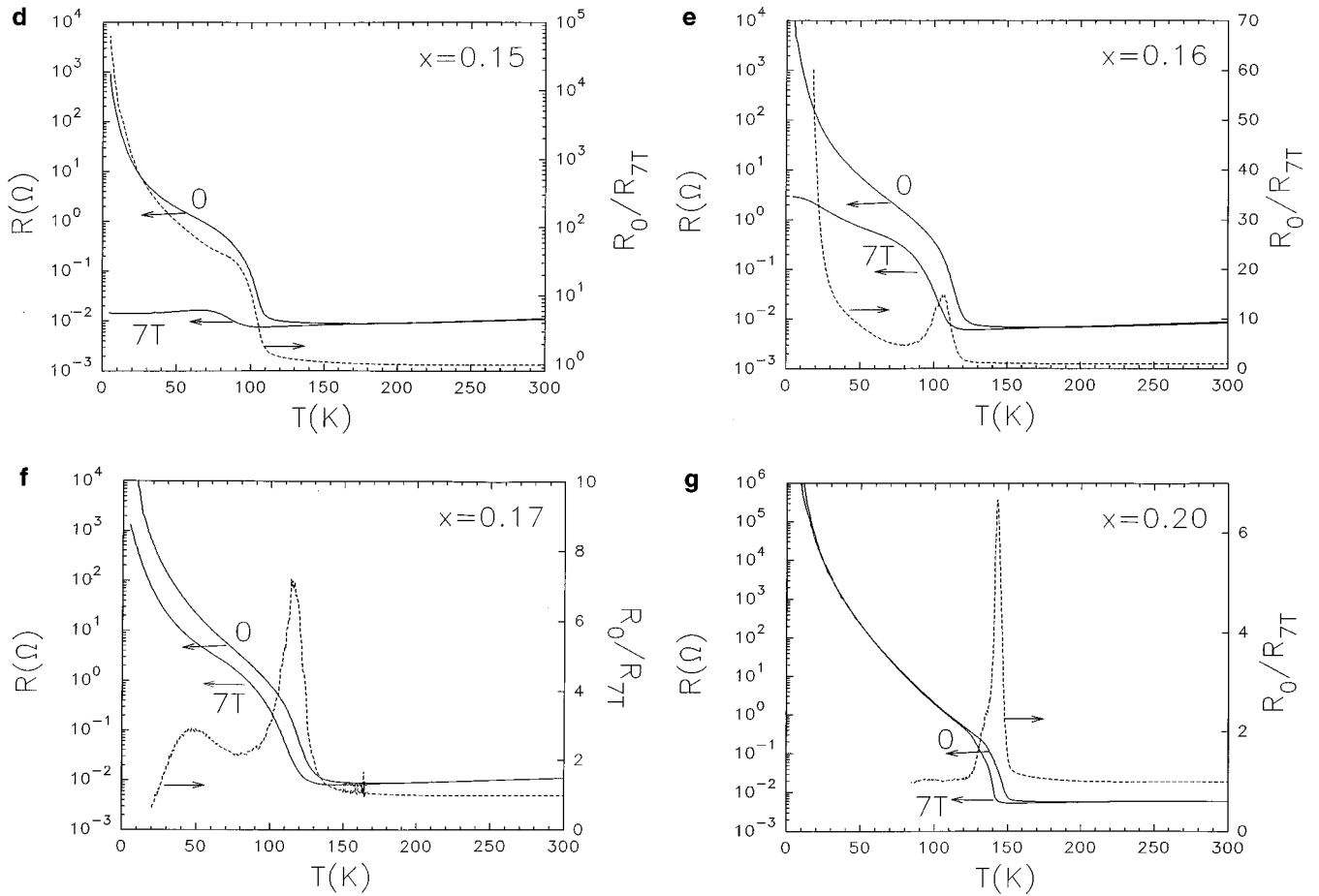
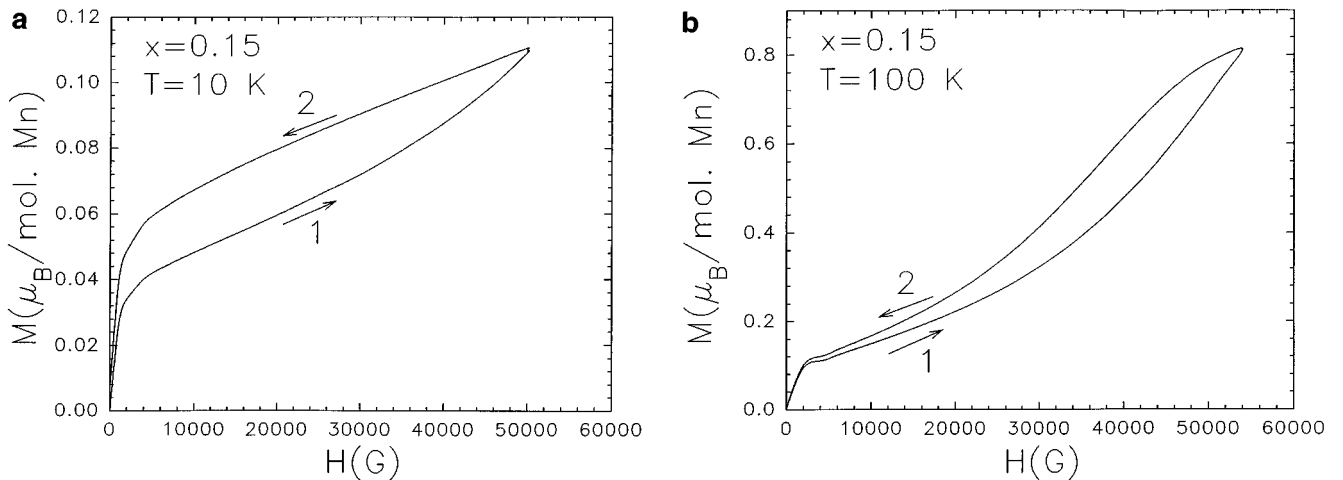


FIG. 3—Continued

magnetic moment of $\sim 3 \mu_B/\text{Mn}$. The physical properties of $\text{Ca}_{0.85}\text{Sm}_{0.15}\text{MnO}_3$ may be explained via a double exchange (DE) model (15). The magnetic field application

reinforces the ferromagnetic component, so that the carrier scattering decreases, thereby inducing negative magnetoresistance.

FIG. 4. Magnetic field dependence of the magnetization M for $\text{Ca}_{0.85}\text{Sm}_{0.15}\text{MnO}_3$ ($x=0.15$) at 10 K (a) and 100 K (b).

REFERENCES

1. R. Von Helmolt, J. Wecker, T. Lorenz, and K. Samwer, *Appl. Phys. Lett.* **67**, 2093 (1995).
2. R. Mahesh, R. Mahendiran, A. K. Raychaudhuri, and C. N. R. Rao, *J. Solid State Chem.* **114**, 297 (1995).
3. A. Urushibara, Y. Moritomo, T. Arima, A. Asamitsu, G. Kido, and Y. Tokura, *Phys. Rev. B* **20**, 14103 (1995).
4. R. Mahendiran, R. Mahesh, A. K. Raychaudhuri, and C. N. R. Rao, *Solid State Commun.* **94**, 515 (1995).
5. V. Caignaert, A. Maignan, and B. Raveau, *Solid State Commun.* **95**, 357 (1995).
6. A. Maignan, V. Caignaert, Ch. Simon, M. Hervieu, and B. Raveau, *J. Mater. Chem.* **5**, 1089 (1995).
7. B. Raveau, A. Maignan, and Ch. Simon, *J. Solid State Chem.* **117**, 424 (1995).
8. R. Mahendiran, S. K. Tiwary, A. K. Raychaudhuri, T. V. Ramakrishnan, R. Mahesh, N. Rangavittal, and C. N. R. Rao, *Phys. Rev. B* **53**, 3348 (1996).
9. A. Maignan, C. Michel, M. Hervieu, and B. Raveau, *Solid State Commun.* **101**, 277 (1997).
10. Z. Jirak, S. Krupicka, Z. Simsa, M. Dlouha, and S. Vratislav, *J. Magn. Mater.* **53**, 153 (1985).
11. P. G. Radaelli, D. E. Cox, M. Marezio, and S. W. Cheong, *Phys. Rev. B* **55**, 3015 (1997).
12. H. Chiba, M. Kikuchi, K. Kusaba, Y. Muraoka, and Y. Syono, *Solid State Commun.* **99**, 449 (1996).
13. Y. Murakami, D. Shindo, H. Chiba, M. Kikuchi, and Y. Syono, *Phys. Rev. B* **55**, 1 (1997).
14. E. O. Wollan and W. C. Koehler, *Phys. Rev. B* **100**, 545 (1955).
15. P. G. de Gennes, *Phys. Rev.* **118**, 141 (1960).